ACCOUNTS
of chemical research

Electron Microscopy Study of Gold Nanoparticles Deposited on Transition Metal Oxides

TOMOKI AKITA,*,† MASANORI KOHYAMA,† AND MASATAKE HARUTA‡

†*Research Institute for Ubiquitous Energy Devices, National Institute of Advanced Industrial Science and Technology (AIST), 1-8-31 Midorigaoka, Ikeda, Osaka 563-8577, Japan, and* ‡*Department of Applied Chemistry, Graduate School of Urban Environmental Sciences, Tokyo Metropolitan University, 1-1 minami-osawa, Hachioji, Tokyo 192-0397, Japan*

RECEIVED ON SEPTEMBER 3, 2012

CONSPECTUS

Many researchers have investigated the catalytic performance of gold nanoparticles (GNPs) supported on metal oxides for various catalytic reactions of industrial importance. These studies have consistently shown that the catalytic activity and selectivity depend on the size of GNPs, the kind of metal oxide supports, and the gold/metal oxide interface structure. Although researchers have proposed several structural models for the catalytically active sites and have identified the specific electronic structures of GNPs induced by the quantum effect, recent experimental and theoretical studies indicate that the perimeter around GNPs in contact with the metal oxide supports acts as an active site in many reactions. Thus, it is of immense importance to investigate the detailed structures of the perimeters and the contact interfaces of gold/metal oxide systems by using electron microscopy at an atomic scale.

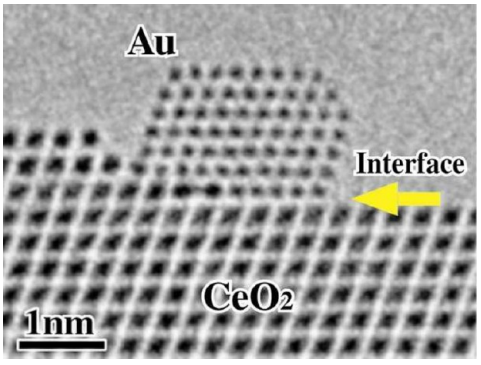

This Account describes our investigation, at the atomic scale using electron microscopy, of GNPs deposited on metal oxides. In particular, high-resolution transmission electron microscopy (HRTEM) and high-angle annular dark-field scanning transmission electron microscopy (HAADF-STEM) are valuable tools to observe local atomic structures, as has been successfully demonstrated for various nanoparticles, surfaces, and material interfaces. TEM can be applied to real powder catalysts as received without making special specimens, in contrast to what is typically necessary to observe bulk materials. For precise structure analyses at an atomic scale, model catalysts prepared by using well-defined single-crystalline substrates are also adopted for TEM observations. Moreover, aberration-corrected TEM, which has high spatial resolution under 0.1 nm, is a promising tool to observe the interface structure between GNPs and metal oxide supports including oxygen atoms at the interfaces. The oxygen atoms in particular play an important role in the behavior of gold/metal oxide interfaces, because they may participate in catalytic reaction steps. Detailed information about the interfacial structures between GNPs and metal oxides provides valuable structure models for theoretical calculations which can elucidate the local electronic structure effective for activating a reactant molecule. Based on our observations with HRTEM and HAADF-STEM, we report the detailed structure of gold/metal oxide interfaces.

1. Introduction

Although gold in bulk is chemically inert, it exhibits high catalytic activities and unique selectivities for various reactions.[1−6] The most critical factor for high catalytic activity is the size of gold particles, which should be smaller than 10 nm in diameter (nanoparticles). The change of electronic structure by the quantum size effect happens when the diameter is smaller than 2 nm (clusters). Recently, it has been proved that the perimeter around GNPs is the site for CO oxidation at and below room temperature.[2,4,7−9] In this mechanism, the size effect can be simply correlated to the length of perimeter region. The quantum size effect is not necessary for the genesis of high catalytic activity for CO oxidation.

The size effect of gold has also been reported for the epoxidation of propylene at around 2 nm.[10−12] In the

Published on the Web 06/18/2013 www.pubs.acs.org/accounts
10.1021/ar300259n

presence of H_2 and O_2, GNPs on Ti-based oxides produce propylene oxide (PO), whereas gold clusters on Ti-based oxides produce propane. In the presence of H_2O and O_2, only gold clusters can produce PO whereas GNPs produce acrolein and CO_2. The reaction of propylene is sensitive to the size of gold particles owing to the quantum size effect and produces different reaction products. The character of the metal oxide supports are also an important factor for these reactions because selective oxidation intermediates (hydroperoxide) should be generated near the perimeter interfaces around GNPs. The Au/metal oxide interface is again essential for the selective oxidation of hydrocarbons over gold catalysts. Typical metal oxide supports and typical reactions catalyzed by GNPs on them are listed in Table 1S in the Supporting Information.

A constraint is that it is difficult to estimate the interface structure of GNPs and metal oxides with a high spatial resolution. Scanning probe microscopy (SPM) is a powerful technique to observe the surface structure with a high spatial resolution[13−15] and enables us to observe atomic gold or a few layers of gold on clean flat metal oxide supports. However, SPM cannot access the perimeter region of GNPs which is constructed at an atomic scale.

X-ray based techniques are also useful to estimate fine structures. However, it is also difficult to detect the information of local structure such as contact interfaces or perimeters around GNPs, because they cover only tiny region against the whole sample area. Moreover, the measurement technique provides spatially averaged information over the whole sample area and therefore needs strictly uniform samples. Theoretical calculations also struggle to form sufficiently detailed model structures which reflect the actual structures of gold catalysts.

Transmission electron microscopy (TEM) is one of the promising methods to observe the interface structure at an atomic scale. TEM has a great advantage that it is applicable to real powder catalysts with high resolution. It can also be used for observing model catalyst structures. A disadvantage of TEM is that the observations should be carried out under high vacuum conditions. Environmental TEM technique can recently overcome such a disadvantage and high resolution observations under various reaction gas atmosphere have been reported for many catalysts.[16−21] In this Account, we will focus on the atomic structure of gold−metal oxide interfaces observed by electron microscopic techniques. Gold is the best sample for TEM analyses since its unique heterogeneous catalysis comes out of the supports and the size and contact structure of GNPs and it gives stronger contrast against the background elements of base metal oxide supports than the other metals.

2. TEM and HAADF-STEM Observation of Gold Particles Deposited on Transition Metal Oxides

TEM is generally used to estimate the dispersion (homogeneous or heterogeneous) of GNPs. It provides not only the mean diameter of particles but also that distribution of diameter. That feature has hardly been applied to the actual characterization of catalysts and only mean diameter is usually used to discuss the catalytic activity. If the catalytic property of GNPs and clusters remarkably changes depending on the specific size, the diameter distribution of GNPs will bring valuable information.

Figure 1 shows low magnification and high magnification TEM images of Au/TiO_2 and Au/CeO_2 prepared by deposition precipitation (DP) method and Au/Fe_2O_3 prepared by coprecipitation (CP) method. Nanosize gold particles are uniformly dispersed on the metal oxide supports. High resolution TEM (HRTEM) images showed truncated polyhedral GNPs, which had low index facets such as (111) and (100), were deposited on the metal oxides. For the GNPs, (110) face was hardly observed. Truncated polyhedral structure was often observed for small GNPs under 10 nm and larger gold particles tended to have equilibrium round shape. The presence of truncated shape means that adhesion energy is relatively strong between gold and the oxide support. The adhesion energy can be estimated from the shape of particle based on the Young-Dupre relationship which is a formula to describe the relations of surface energy, interfacial energy and contact angle of particle and substrate.[22] The multitwinned particles[23,24] were also observed when gold particles become large.

A variety of interface structures can be assumed for the gold−metal oxide interfaces since there are many types of combinations between gold faces and metal oxide surfaces in actual catalysts and metal oxide supports are also particles which have various crystal faces. Accordingly, only typical low index interfaces have been studied as model structures in surface science approaches and theoretical calculations. Some orientation relationships were observed by HRTEM for Au/TiO_2[25] and Au/CeO_2.[26] Several preferential orientation relationships were also observed, $Au(111)//TiO_2(110)$ for Au/rutile TiO_2, $Au(111)//TiO_2(112)$ for anatase TiO_2, and $Au(111)//CeO_2(111)$. These results were confirmed by observing several GNPs by HRTEM, however, the static approach should be done in order to estimate the preferential orientation relationships and stable structures. Since TEM focuses on

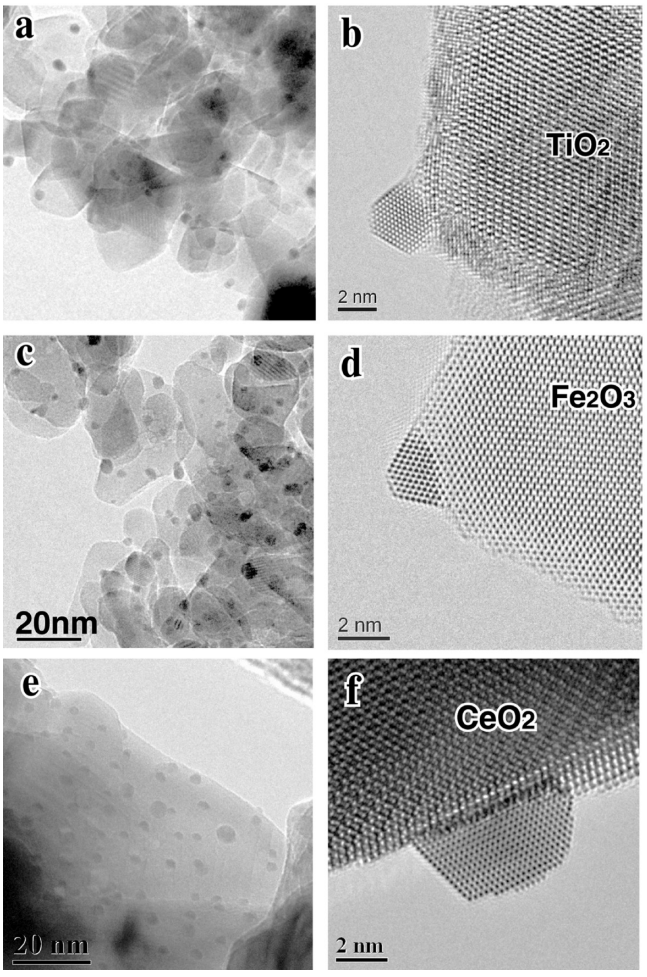

FIGURE 1. Typical low-magnification and high-magnification TEM images of a Au/TiO_2 catalyst (a, b) prepared by deposition precipitation method (DP), a Au/Fe_2O_3 catalyst (c, d) prepared by coprecipitation method, and a Au/CeO_2 catalyst (e, f) prepared by deposition precipitation method using low surface area CeO_2 support.

the local structure, the observations should be carried out at random for various areas as many as possible. In order to make reasonable structure models for the first principle calculations, it is necessary to elucidate the interface structures by TEM at an atomic scale.

HAADF-STEM technique is widely used to observe GNPs because the contrast is improved with an increase in the Z number of an element. It can detect even small gold clusters because gold is a heavy atom which has strong scattering factor for electrons.[27] Figure 2 shows an example of HAADF-STEM image of Au/Fe_2O_3 catalyst. In low magnification image, GNPs can be detected with bright contrast. The HAADF-STEM image has a great advantage that the images are not disturbed by diffraction contrast or phase contrast which happens in normal TEM images. The contrast of HAADF-STEM image depends on the element and thickness of sample.

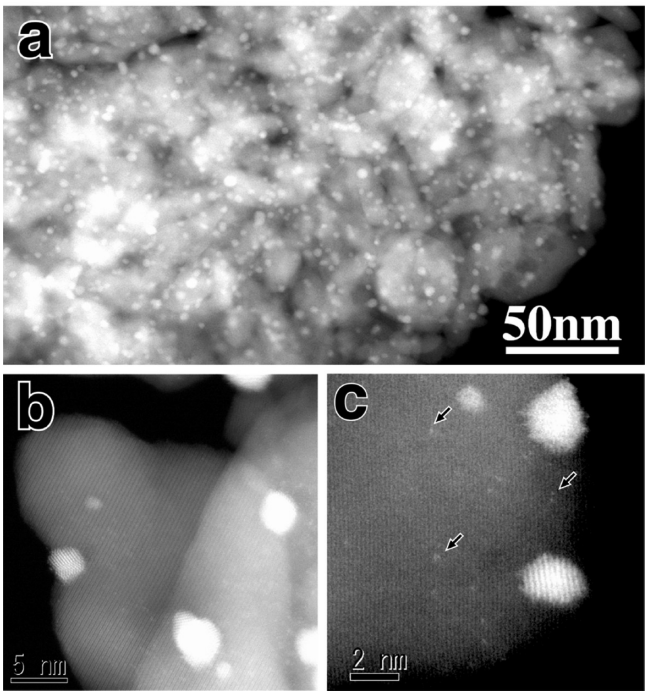

FIGURE 2. HAADF-STEM images of a Au/Fe_2O_3 catalyst prepared by coprecipitation method. Low magnification image (a) and high magnification images (b, c).

Even single gold atoms can be detected in high magnification and high signal-to-noise ratio,[28−31] if the mean *Z* number of the support material is small and thin enough.

Catalytic properties of size selected gold clusters are interesting subjects.[32] Not only the measurement of the size of GNPs but also the estimation of the number of gold atoms in tiny gold clusters will become an important subject in the future catalysis research. Many small gold clusters were observed in the Au/Fe_2O_3 catalyst prepared by CP method but through slow addition of an aqueous alkali solution into an aqueous solution of $HAuCl_4$ (opposite to the procedure for Figure.2). The correlation between gold clusters or atoms and catalytic activity are discussed,[29] suggesting that the gold clusters or isolated gold atoms might be responsible for the high catalytic activity for CO oxidation. In contrast, in the case of Au/TiO_2 prepared by DP method, although the single atoms were hardly observed, the catalysts exhibited high catalytic activity.[33] The details of this difference will be discussed in the near future based on the various data obtained by aberration corrected HAADF-STEM.

Some advanced studies have been carried out to estimate the number of atoms in metal clusters by quantification of the image intensity of HAADF-STEM.[34,35] It is also an indispensable method to observe the interface structure in atomic scale. The atomic column positions in gold and support

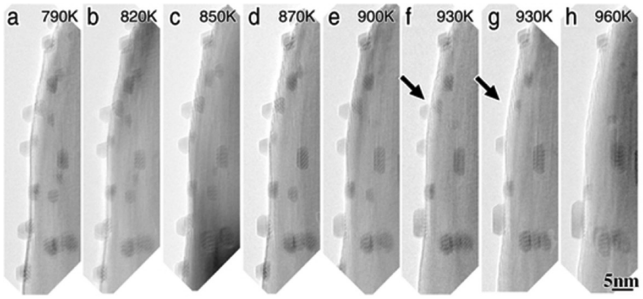

FIGURE 3. HRTEM images of GNPs deposited on CeO_2 by DP during the course of heating in TEM at: 790 K (a), 820 K (b), 850 K (c), 870 K (d), 900 K (e), 930 K (f,g), and 960 K (h).

crystals can be observed directly by HAADF-STEM method while the HRTEM images need complicated image simulations for the determination of atomic column positions.[27]

The interface structure between gold and metal oxide is crucial for the genesis of catalysis,[2,4−8] in particular, oxygen molecule activation and hydrogen molecule dissociation. The stoichiometry of the oxide support defines the electronic structure at perimeter interfaces;[36] moreover, the oxygen defects around perimeter may directly participate in catalytic reactions. Direct observation of oxygen vacancies is very important to study the role of the perimeter interface in gold−metal oxide systems, but it is still very difficult even by using the advanced microscopic technique.

3. Growth of Gold Particles on Metal Oxide

Stability of GNPs on metal oxide is crucial for maintaining them small and catalytically active for a long period. The growth of GNPs on metal oxides was observed for TiO_2, CeO_2 and other oxides.[37−39] Gold nanoparticles usually grow by Ostwald ripening process on metal oxide surfaces. Figure 3 shows the TEM images obtained during heating the Au/CeO_2 catalyst in an electron microscope from 790 to 960 K. It is apparent that the GNPs became larger on a CeO_2 particle, but the location of larger GNPs did not change during the heating process. Smaller GNPs disappeared as indicated by arrows in Figure 3 when heating temperature was raised. Gold atoms might diffuse on the metal oxide surfaces during growth while the movement of single gold atoms could not be detected by TEM. In order to keep gold clusters small in real catalysts, geometrical defects such as atomic steps on the support surfaces and grain boundaries between support particles are necessary.

It is interesting that the growth of GNPs on oxide supports can be suppressed by heating in a stream containing hydrogen atmosphere.[40,41] In reductive atmosphere, oxygen defects can be created on the metal oxide surfaces and the defect sites prevent the diffusion of gold atoms and particles to some extent because the adhesion energy is generally larger over oxygen defective surfaces.[36]

The DP method, which is the most popular technique to prepare supported gold catalyst is sensitive to the surface charge of metal oxide supports in aqueous solution of gold precursors. In principle, on acidic metal oxides, the isoelectric point (IEP) of which is below pH 6 (the surface charge is negative above pH 6), $Au(OH)_3$ cannot be deposited, whereas on basic metal oxides with the IEP above pH 7 (the surface charge is positive above pH 7) $Au(OH)_3$ can be efficiently deposited. The population of gold particles after drying before calcination is different for each particle of TiO_2 (Degussa P-25) which contains rutile and anatase TiO_2 crystals. The solid gold precursor which was identified as $Au(OH)_3$ by means of XPS, and XANES[42] tends to deposit preferentially on the rutile TiO_2 surfaces when both crystals coexist in the support.[38] This tendency was also confirmed for the TiO_2 powder which was artificially prepared by physical mixing of rutile and anatase TiO_2. Figure 4 shows the HAADF-STEM image of GNPs deposited by DP method on a physical mixture of rutile and anatase TiO_2 particles before calcination. The population of GNPs is apparently different for left and right TiO_2 particles. Because the isoelectric point or point of zero charge of support powder in aqueous solution is not different between anatase and rutile TiO_2 (around pH 6).[43] The chemical interaction between TiO_2 support and $Au(OH)_4^-$ ions are different for rutile and anatase.

The electron energy loss spectroscopy (EELS) analysis proves the crystalline structure by using O−K edge energy loss near edge structure (ELNES) shown in Figure 4b. As shown by an arrow, the characteristic feature of crystal appeared in the ELNES of O−K edge which reflects the unoccupied density of state of the TiO_2 crystal.[44] Since the crystalline structure can be determined by these O−K edge EELS spectra, it is obvious that gold precursor tends to be deposited preferentially on rutile TiO_2 during DP in $HAuCl_4$ aqueous solution.

4. Interface Structure between Gold and Metal Oxides

Figure 5 shows the profile-view HAADF-STEM image of a GNP on CeO_2 polycrystalline substrate which was prepared as a model structure by vacuum deposition method.[45] The atomically resolved profile-view HAADF-STEM was obtained and the interface structure between GNP and CeO_2 was also observed at an atomic resolution. The preferential orientation relationship of $Au(111)[1\bar{1}0]//CeO_2(111)[1\bar{1}0]$ is often

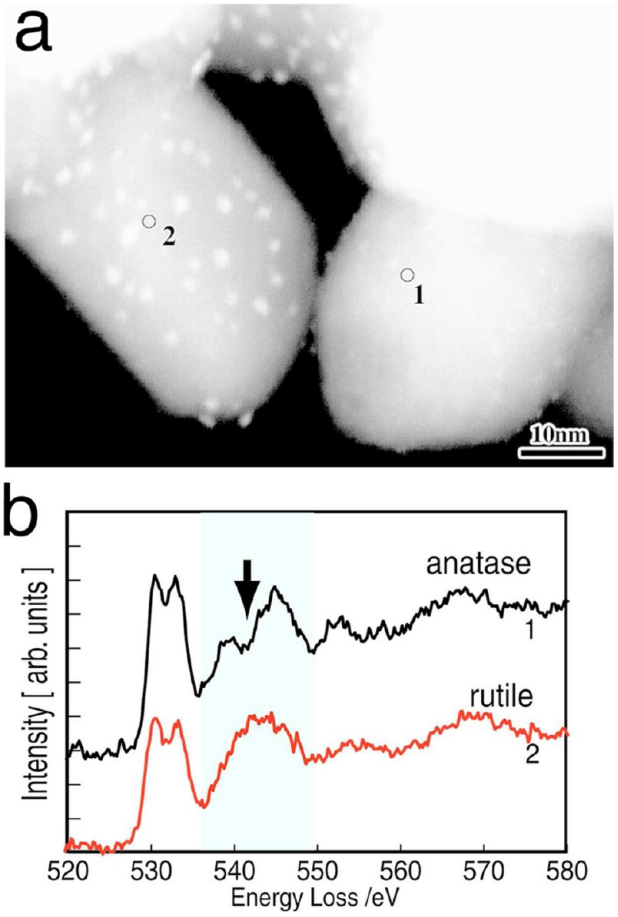

FIGURE 4. ADF-STEM image (a) of GNPs on a physical mixture of rutile and anatase TiO_2 and O−K edge EELS spectra (b) obtained from each numbered site of TiO_2 particle.

observed for the Au/CeO_2 interface as observed for the Au/CeO_2 powder catalysts prepared by DP method.[26] The lattice constant of gold and CeO_2 is 0.40782 and 0.5411 nm, respectively, and the lattice mismatch is 28%. The interface has an incoherent configuration with a nearly 4:3 coincidence relation, due to the relation of lattice parameters of gold and CeO_2 as approximately $4a_{Au} = 3a_{CeO2}$. The distance between gold atomic layer and cerium atomic layer at the interface is directly estimated to be 0.28 nm from the HAADF-STEM image.[46] This distance suggests that the oxygen atomic layer is absent at the Au/CeO_2 interfaces. The distance value does not contradict the stable distance between gold and oxygen deficient $CeO_2(111)$ surface obtained by the first principle calculations of gold atomic layer on oxygen deficient $CeO_2(111)$.[47]

Gold particles often exhibit reconstructed structure at {100} surface as observed in Figure 5. The gold particle is surrounded by (111) and (100) surfaces. The atomic arrangement of Au(100) surface is illustrated in Figure 5c, whereas the excess atomic column is observed and arrangement is

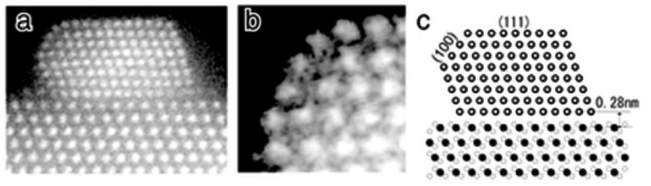

FIGURE 5. Profile-view HAADF-STEM image of GNP deposited on CeO_2 poly crystalline substrate by vacuum deposition (a). Enlarged image of the Au(100) surface (b) and the corresponding model structure (c). Reproduced with permission from ref 45. Copyright 2010 Trans Tech Publications, Switzerland.

disordered in Figure 5b. The Au(100) reconstructed surface is usually observed for the clean Au(100) surface which is formed under well-defined condition under ultra high vacuum (UHV) or electro chemical reactions.[48−50] The reconstructed structure is often observed by TEM for nanoparticles,[49] but it is actually not stable and fluctuated by electron beam irradiation during TEM or HAADF-STEM observations. This means that the local area of nanoparticle can be temporarily cleaned up by electron beam irradiation during observation.

Gold nanoparticle itself is not stable at room temperature and the structure change occurs easily during TEM observation by electron beam irradiation.[26,47,51] Figure 6 shows sequential images of GNPs during HAADF-STEM observations. The gold particle became smaller during observation.[47] In contrast, as shown in Figure 6e and f, the gold particle became larger while the electron beam irradiation is stopped. The three-dimensional (3D) shape is also estimated from the intensity profile of HAADF-STEM image as presented in Figure 6. The intensity of the HAADF-STEM image is almost proportional to the thickness of the thin sample. By taking the intensity profile crossing the HAADF-STEM image of GNPs, the position of edge can be detected from the maximum intensity in the profile. The 3D shape can be deduced from the intensity profile of HAADF-STEM, and the number of atoms in a particle can also be estimated.

The number of atoms can be estimated if the condition that symmetry of the particle is fulfilled to some extent. The correlation between the thickness of the atomic column and the image intensity, which is shown in Figure 7, can distinguish the number of atoms in an atomic column along beam direction with accuracy of a few atoms. For example, Figure 7 shows, at the perimeter interface the disordered structure which is deviated from the ideal position of fcc gold crystal. This is not a single gold atom since the intensity is much stronger. The number of gold atoms at this atomic column along beam direction is estimated to be 5 ± 1 atoms, which indicate the periodicity of the coincidence lattice between

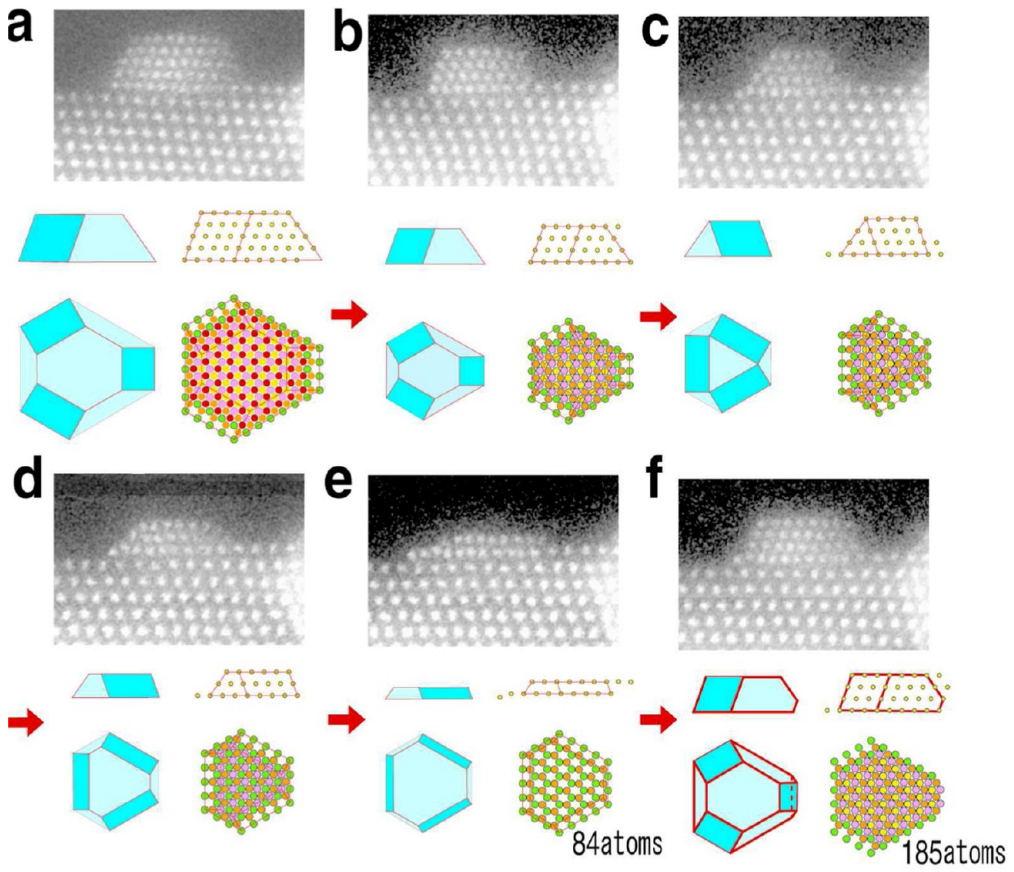

FIGURE 6. Sequential HAADF-STEM images of a GNP deposited on CeO_2 during structure change by electron beam irradiation (a–f) and the corresponding three-dimensional particle shape of each GNP estimated from the intensity profiles of HAADF-STEM images.

gold and CeO_2. The number of gold atoms contained in the particle can be estimated to be 80 atoms in Figure 6e, and 180 atoms in Figure 6f. These results indicate that about 100 gold atoms disappeared from the gold particle and come back to the original gold particle during 15 min interruption of electron beam. It can be assumed that gold atoms are dispersed over the CeO_2 surfaces during the electron beam irradiation. Gold atoms might be trapped at oxygen defect of CeO_2 sites when the reductive condition is given, for example, electron beam irradiation. Gold atoms can be released from the defect site when the oxidative conditions are given and stoichiometric CeO_2 surfaces are formed.

5. Aberration Corrected TEM Images

Oxygen is a key element when we discuss the reaction mechanism of oxidation on gold catalysts, which are extraordinarily active at low temperature and selective for many reactions in gas and liquid phases.[52] Because HAADF-STEM cannot directly observe the light atoms such as oxygen, aberration corrected HRTEM is very useful to observe the oxygen atoms at perimeter or contact interfaces between gold and the metal oxide support with a high spatial resolution.[53] Currently, oscillation of the phase contrast transfer function and complicated contrasts can also be suppressed.[53]

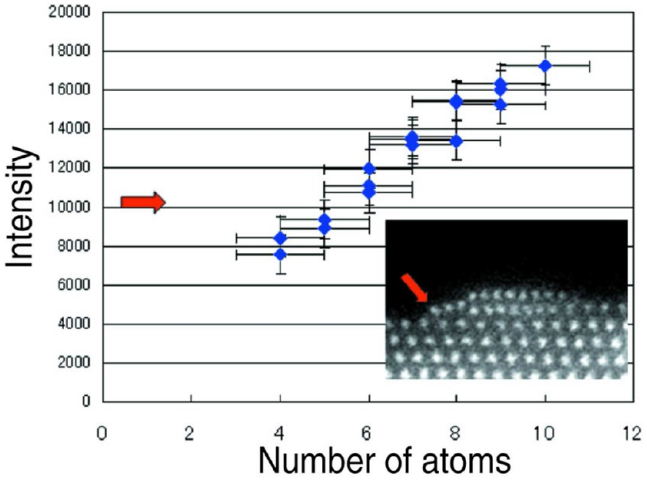

FIGURE 7. Relation of the number of atoms in each atomic column in GNP deposited on CeO_2 by vacuum deposition and the signal intensity of the atomic column in HAADF-STEM image. Red arrow in the graph corresponds to the intensity of the Au atomic column indicated by red arrow in superimposed HAADF-STEM image.

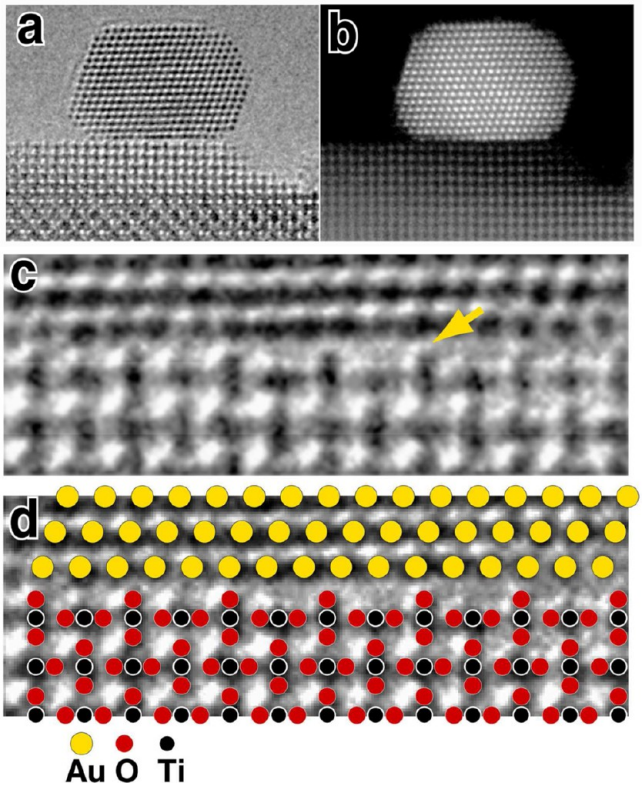

FIGURE 8. Aberration corrected TEM (a) and HAADF-STEM image (b) of a GNP deposited on TiO_2 (110) by DP, and enlarged aberration corrected TEM image of the interface (c) and the corresponding model structure (d) indicating the position of atomic columns of Au (yellow), Ti (black), and O (red) viewed along TiO_2[001].

Figure 8 shows the HRTEM image and HAADF-STEM image of the interface between a GNP and rutile TiO_2 which was prepared by DP method using large TiO_2 particles. The incident electron beam direction is parallel to the [001] zone axis for TiO_2 and [110] zone axis for gold crystal. The gold particle is supported on the TiO_2(110) surface with the orientation relationship of Au(111)[110]//TiO_2(110)[001].

The distance between gold atomic layer and titanium layer was estimated to be 0.33 nm by HAADF-STEM image, as shown in Figure 8b. The distance agreed with the result which was previously obtained for GNPs on single crystalline TiO_2 substrate prepared by vacuum deposition.[54] The HRTEM image resolved the interface structure with atomic scale as shown in Figure 8c and the structure model is superimposed in Figure 8d. The bridging oxygen on TiO_2(110) surface is observed, as indicated by arrow. This means that the GNP was deposited on the stoichiometric TiO_2(110) surface. The apparent distortion is not observed in gold atomic layer, meaning that the interaction between gold and TiO_2 surface is not so strong.

Gold/NiO interface was also observed by TEM and HAADF-STEM. The model structure of GNPs on NiO was

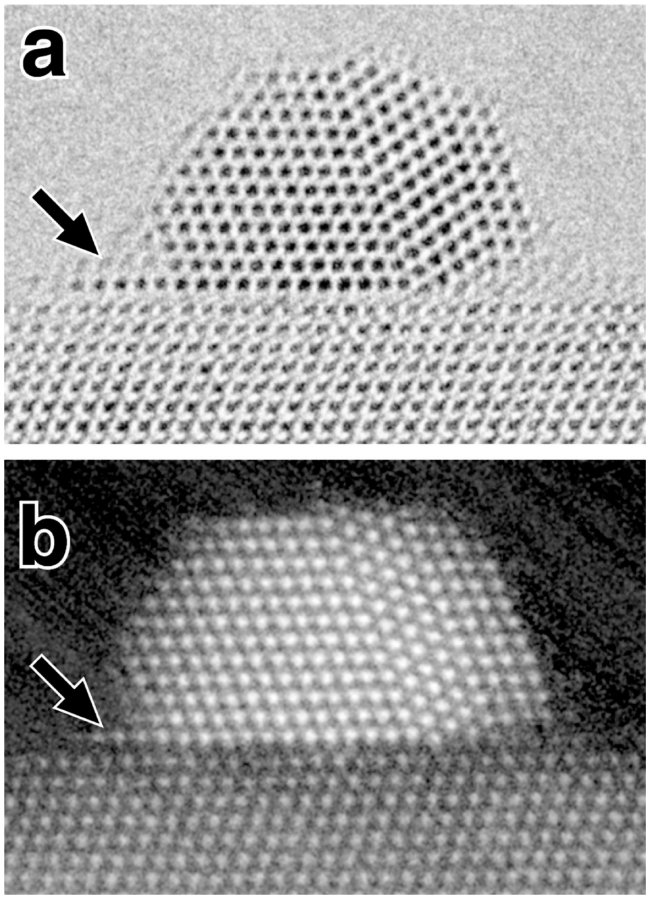

FIGURE 9. Aberration corrected TEM (a) and HAADF-STEM image (b) of a GNP deposited on NiO by vacuum deposition.

prepared by vacuum deposition method. Small gold particles of approximately 2−5 nm in diameter were deposited on the edge of NiO polycrystalline substrate with sufficiently high population in this experiment. Gold particles also tend to be deposited on the NiO surfaces with the preferential orientation relationships of (111)[1$\bar{1}$0]Au//(111)[1$\bar{1}$0]NiO or (111)[$\bar{1}$10]Au//(111)[1$\bar{1}$0]NiO for the NiO(111) surface. The tendency of orientation relationship was estimated for 303 GNPs in HRTEM images, and gold particles with the orientation relationship of (111)[1$\bar{1}$0]Au//(111)[1$\bar{1}$0]NiO and (111)[$\bar{1}$10]Au//(111)[1$\bar{1}$0]NiO occupied 63%. The lattice constant of Au and NiO is 0.40782 nm and 0.41946 nm, respectively. The lattice mismatch is only 2% and the epitaxial relation is simply due to the lattice matching at interface.

Figure 9a and b shows aberration corrected HRTEM and HAADF-STEM images for a GNP on NiO(111), respectively. The incident electron beam direction was set along the NiO [1−10] zone axis and the interface structure could be observed clearly. Although the GNP includes the defect structure, they are also deposited with the orientation relationship of (111)[$\bar{1}$10]Au//(111)[1$\bar{1}$0]NiO. From the HAADF-STEM

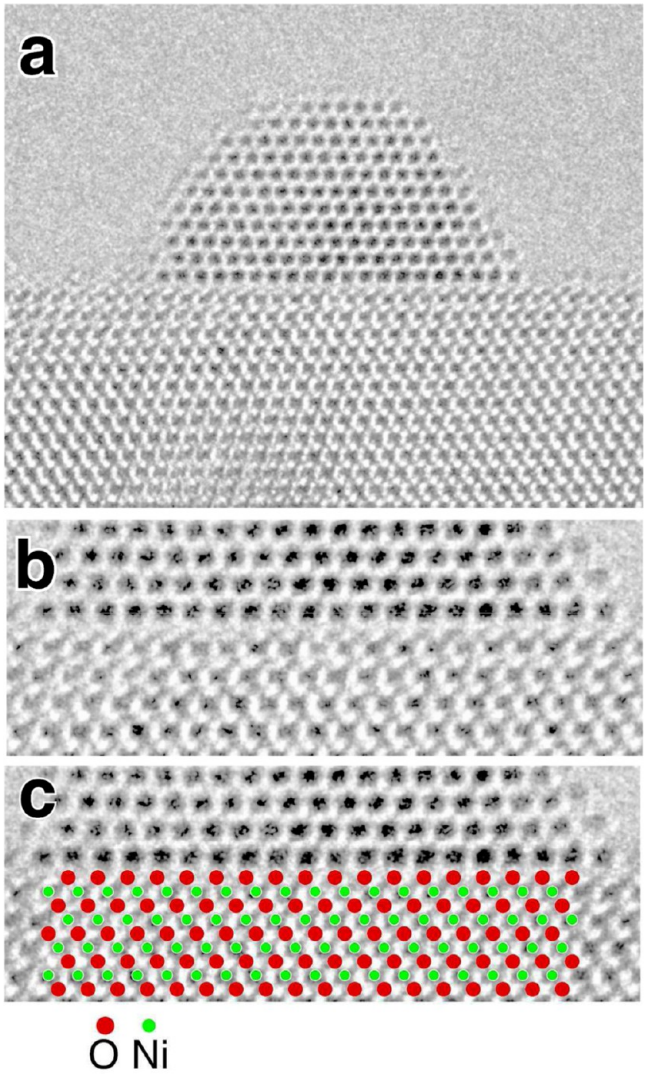

FIGURE 10. Aberration corrected TEM image of GNP deposited on NiO(111) by vacuum deposition (a), enlarged TEM image of the interface (b), and a corresponding structure model (c) indicating the atomic column position of Ni (green) and O (red) viewed along the NiO ⟨110⟩ direction.

image, the distance between gold and nickel atom layers at the interface was estimated to be 0.32 ± 0.01 nm. This distance suggests that the oxygen terminated surface is formed at the Au/NiO(111) interface. In addition, gold monolayer is formed at around the perimeter as indicated by an arrow. This feature is similar to GNP on CeO_2 shown in Figure 6. This structure indicated that the adhesion energy is relatively strong between Au and NiO at this perimeter region. Although it is not clear from the image whether gold monolayer is formed on oxygen atoms, the structure seems to be formed by removing the surface oxygen atoms by electron beam irradiation and the region has strong adhesion energy as observed in the case of Au on CeO_2.[47]

Aberration corrected TEM images of Au/NiO interface are shown in Figure 10. The HRTEM image of the interface indicates that the oxygen atom layer exists at the interface. The dark contrast appears at the Au/NiO interface corresponding to oxygen position of NiO crystal. The structure model of gold and NiO is superimposed in Figure 10c. The TEM image suggests that GNP is supported on the oxygen terminated NiO(111) surface.

The electron microscopic observations described above are carried out in the static conditions in a vacuum chamber. Of course, structural observation of heterogeneous catalysts should be done under reaction conditions in order to elucidate the effective structure for catalytic reactions.[18,55]

6. Conclusions

The fine structures of the interfaces between gold nanoparticles (GNPs) and transition metal oxides such as TiO_2, Fe_2O_3, NiO, and CeO_2 were observed at an atomic scale by TEM techniques. Since it has been proved that CO oxidation and H_2 dissociation takes place at the perimeter interface, their atomic scale structures are of immense importance to understand the catalytic properties. The interface was observed by TEM, and the atomic structures including oxygen could be observed by aberration corrected HRTEM which have already been commercially available. The observations should be carried out for many gold particles in order to obtain rational conclusions about the ruling structure of GNPs on metal oxides. Many high quality images of the gold catalysts will be reported in the near future. The observations should also be done for the catalysts after various pretreatments and under the presence of reactant gases. Of course, the final target is to elucidate the correlation between fine structures in atomic scale under reaction conditions and actual catalytic properties.

Supporting Information. Table showing the selection of transition metal oxides as supports for gold catalysts and related references. This material is available free of charge via the Internet at http://pubs.acs.org.

BIOGRAPHICAL INFORMATION

Tomoki Akita received his Ph.D. from Osaka University in 1998. After working as a postdoctoral researcher for one year at Osaka National Research Institute (ONRI), he was employed as permanent staff by ONRI. He is now a senior research scientist at the Research Institute for Ubiquitous Energy Devices, National Institute for Advanced Science and Technology (AIST). He has interests in atomic scale characterization of functional materials such as catalysts, electrodes for batteries and fuel cells by using electron microscopy.

Masanori Kohyama is a principle scientist in the Research Institute for Ubiquitous Energy Devises, AIST. He graduated from the master's course of the University of Tokyo in 1984 and received Doctor of Engineering in 1992 from the University of Tokyo. He joined ONRI in 1985. He became Leader of Interface Science Research Group in Special Division of Green Life Technology, AIST in 2001, and Leader of Material Science Research Group in Research Institute for Ubiquitous Energy Devises, AIST in 2004. He is engaged in first-principles calculations of materials interfaces, the development of computer programs of first-principle calculations, collaboration technology between TEM observation and theoretical calculations. He received Distinguished Achievement Award of the Japan Institute of Metals in 2001, and became Fellow of the Institute of Physics (U.K.) in 2004.

Masatake Haruta obtained a B.S. degree from Nagoya Institute of Technology in 1970 and a Doctor of Engineering from Kyoto University in 1976. He began his independent career at ONRI in 1976. Since then he has been involved in catalysis research, in particular, catalysis by gold. From October of 1981, he stayed for one year at Universite Catholique de Louvain. In 1990, he was promoted to head of the catalysis section and in 1999 to director of the department of energy and the environment. In 2001, he was appointed the director of Research Institute for Green Technology, AIST at Tsukuba. In April of 2005, he moved to Tokyo Metropolitan University as full professor. The awards Haruta received include 15th Osaka Science Prize (1997), Science Award from Catalysis Society of Japan (2002), Henry J. Albert Award from International Precious Metals Institute (2002), the Chemical Society of Japan Award (2010), Spiers Memorial Award from Royal Society of Chemistry (2011), and 2012 Thomson Reuters Citation Laureate: chemistry (2012).

FOOTNOTES

*To whom correspondence should be addressed. E-mail: t-akita@aist.go.jp.
The authors declare no competing financial interest.

REFERENCES

1 Haruta, M.; Kobayashi, T.; Sano, H.; Yamada, N. Novel Gold Catalysts for the Oxidation of Carbon Monoxide at a Temperature far Below 0 °C. *Chem. Lett.* **1987**, 405–408.

2 Haruta, M. When Gold is not Noble: Catalysis by Nanoparticles. *Chem. Rec.* **2003**, *3*, 75–87.

3 Bond, G. C.; Louis, C.; Thompson, D. T. *Catalysis by Gold*; Imperial College Press: London, 2006.

4 Bond, G. C.; Thompson, D. T. Catalysis by Gold. *Catal. Rev. Sci. Eng.* **1999**, *41*, 319–388.

5 Hashmi, A. S. K. Gold-Catalyzed Organic Reactions. *Chem. Rev.* **2007**, *107*, 3180–3211.

6 Hashmi, A. S. K.; Hutchings, G. J. Gold Catalysis. *Angew. Chem., Int. Ed.* **2006**, *45*, 7896–7936.

7 Haruta, M. Role of Perimeter Interfaces in Catalysis by Gold Nanoparticles. *Faraday Discus.* **2011**, *152*, 11–32.

8 Fijitani, T.; Nakamura, I. Mechanism and Active Sites of the Oxidation of CO over Au/TiO_2. *Angew. Chem., Int. Ed.* **2011**, *50*, 10144–10147.

9 Green, I. X.; Tang, W.; Neurock, M.; Yates, J. T., Jr. Spectroscopic Observation of Dual Catalytic Sites During Oxidation of CO on a Au/TiO_2 Catalyst Science. *Science* **2011**, *333*, 736–739.

10 Hayashi, T.; Tanaka, K.; Haruta, M. Selective Vapor-phase Epoxidation of Propylene over Au/TiO_2 Catalysts in the Presence of Oxygen and Hydrogen. *J. Catal.* **1998**, *178*, 566–575.

11 Qi, C.; Huang, J.; Bao, S.; Su, H.; Akita, T.; Haruta, M. Switching of Reactions between Hydrogenation and Epoxidation of Propene over Au/Ti-based Oxides in the Presence of H_2 and O_2. *J. Catal.* **2011**, *281*, 12–20.

12 Huang, J.; Akita, T.; Faye, J.; Fujitani, T.; Takei, T.; Haruta, M. Propene Epoxidation with Dioxygen Catalyzed by Gold Clusters. *Angew. Chem., Int. Ed.* **2009**, *48*, 7862–7866.

13 Chen, M.; Goodman, D. W. Catalytically Active Gold: From Nanoparticles to Ultrathin Films. *Acc. Chem. Res.* **2006**, *39*, 739–746.

14 Risse, T.; Shaikhutdinov, S.; Nilius, N.; Sterrer, M.; Freund, H. J. Gold Supported on Thin Oxide Films: From Single Atoms to Nanoparticles. *Acc. Chem. Res.* **2008**, *41*, 949–956.

15 Maeda, Y.; Okumura, M.; Tsubota, S.; Kohyama, M.; Haruta, M. Local Barrier Height of Au Nanoparticles on a $TiO_2(110)$-(1×2) surface. *Appl. Surf. Sci.* **2004**, *222*, 409–414.

16 Gai, P. L.; Boyes, E. D. Advances in Atomic Resolution in situ Environmental Transmission Electron Microscopy and a Aberration Corrected in situ Electron Microscopy. *Microsc. Res. Tech.* **2009**, *72*, 153–164.

17 Hansen, P. L.; Wagner, J. B.; Helveg, S.; Rostrup-Nielsen, J. R.; Clausen, B. S.; Topsøe, H. Atom-Resolved Imaging of Dynamic Shape Changes in Supported Copper Nanocrystals. *Science* **2002**, *295*, 2053–2055.

18 Yoshida, H.; Kuwauchi, Y.; Jinschek, J. R.; Sun, K.; Tanaka, S.; Kohyama, M.; Shimada, S.; Haruta, M.; Takeda, S. Visualizing Gas Molecules Interacting with Supported Nanoparticulate Catalysts at Reaction Conditions. *Science* **2012**, *335*, 317–319.

19 Giorgio, S.; Sao Joao, S.; Nitsche, S.; Chaudanson, D.; Sitja, G.; Henry, C. R. Environmental Electron Microscopy (ETEM) for Catalysts with a Closed E-cell with Carbon Windows. *Ultramicroscopy* **2006**, *106*, 503–507.

20 Giorgio, S.; Cabié, M.; Henry, C. R. Dynamic Observations of Au Catalysts by Environmental Electron Microscopy. *Gold Bull.* **2008**, *41*, 167–173.

21 Ueda, K.; Kawasaki, T.; Hasegawa, H.; Tanji, T.; Ichihashi, M. First Observation of Dynamic Shape Changes of a Gold Nanoparticle Catalyst under Reaction Gas Environment by Transmission Electron Microscopy. *Surf. Interface Anal.* **2008**, *40*, 1725–1727.

22 Cosandey, F.; Madey, T. E. Growth, Morphology, Interfacial Effects and Catalytic properties of Au on TiO_2. *Surf. Rev. Lett.* **2001**, *8*, 73–93.

23 Marks, L. D. Experimental Studies of Small Particle Structures. *Rep. Prog. Phys.* **1994**, *57*, 603–649.

24 Koga, K.; Sugawara, K. Population Statistics of Gold Nanoparticle Morphologies: Direct Determination by HREM Observations. *Surf. Sci.* **2003**, *529*, 23–35.

25 Akita, T.; Tanaka, K.; Tsubota, S.; Haruta, M. Analytical High-resolution TEM Study of Supported Gold Catalysts: Orientation Relationship between Au Particles and TiO_2 supports. *J. Electron Microsc.* **2000**, *49*, 657–662.

26 Akita, T.; Okumura, M.; Tanaka, K.; Kohyama, M.; Haruta, M. TEM Observation of Gold Nanoparticles Deposited on Cerium Oxide. *J. Mater. Sci.* **2005**, *40*, 3101–3106.

27 Pennycook, S. J.; Nellist, P. D. *Scanning Transmission Electron Microscopy: Imaging and Analysis*; Springer: New York, 2011.

28 Batson, P. E. Motion of Gold Atoms on Carbon in the Aberration-Corrected STEM. *Microsc. Microanal.* **2008**, *14*, 89–97.

29 Herzing, A. A.; Kiely, C. J.; Carley, A. F.; Landon, P.; Hutchings, G. J. Identification of Active Gold Nanoclusters on Iron Oxide Supports for CO Oxidation. *Science* **2008**, *321*, 1331–1335.

30 Uzun, A.; Ortalan, V.; Hao, Y.; Browning, N. D.; Gates, B. C. Imaging Gold Atoms in Site-Isolated MgO-Supported Mononuclear Gold Complexes. *J. Phys. Chem. C* **2009**, *113*, 16847–16849.

31 Lu, J.; Aydin, C.; Browning, N. D.; Gates, B. C. Imaging Isolated Gold Atom Catalytic Site in Zeolite NaY. *Angew. Chem., Int. Ed.* **2012**, *51*, 5842–5846.

32 Tsunoyama, H.; Tsukuda, T. Magic Numbers of Gold Clusters Stabilized by PVP. *J. Am. Chem. Soc.* **2009**, *131*, 18216–18217.

33 Haruta, M.; Tsubota, T.; Kobayashi, T.; Kageyama, H.; Genet, M. J.; Delmon, B. Low-Temperature Oxidation of CO over Gold supported on TiO_2, α-Fe_2O_3, and Co_3O_4. *J. Catal.* **1993**, *144*, 175–192.

34 Treacy, M. M. J.; Rice, S. B. Catalyst Particle sizes from Rutherford Scattering Intensities. *J. Microsc.* **1989**, *156*, 211–234.

35 Wang, Z. W.; Toikkanen, O.; Yin, F.; Li, Z. Y.; Quinn, B. M.; Palmer, R. E. Counting the Atoms in Supported, Monolayer-Protected Gold Clusters. *J. Am. Chem. Soc.* **2010**, *132*, 2854–2855.

36 Okazaki, K.; Morikawa, Y.; Tanaka, S.; Tanaka, K.; Kohyama, M. Electronic Structures of Au on $TiO_2(110)$ by First-principles Calculations. *Phys. Rev. B* **2004**, *69*, 235404.

37 Campbell, C. T. Ultrathin Metal Films and Particles on Oxide Surfaces: Structural, Electronic and Chemisorptive Properties. *Surf. Sci. Rep.* **1997**, *27*, 1–111.

38 Akita, T.; Lu, P.; Ichikawa, S.; Tanaka, K.; Haruta, M. Analytical TEM Study on the Dispersion of Au Nanoparticles in Au/TiO_2 Catalyst Prepared under Various Temperatures. *Surf. Interface Anal.* **2001**, *31*, 73–78.

39 Akita, T.; Tanaka, T.; Kohyama, M.; Haruta, M. Analytical TEM Study on Structural Changes of Au Particles on Cerium Oxide using a Heating Holder. *Catal. Today* **2007**, *122*, 233–238.

40 Akita, T.; Tanaka, T.; Kohyama, M.; Haruta, M. TEM and STEM study of the Au nanoparticles Supported on Metal Oxides. *Mater. Res. Soc. Symp. Proc.* **2008**, *1026*, C17–14.

41 Zanella, R.; Louis, C. Influence of the Conditions of Thermal Treatments and of Storage on the Size of the Gold Particles in Au/TiO_2 samples. *Catal. Today* **2005**, *107–108*, 768–777.

42 Kageyama, H.; Tsubota, S.; Kadono, K.; Fukumi, K.; Akai, T.; Kamijo, N.; Haruta, M. XAFS Study on Chemistry in Preparation of Au/TiO_2 and Au/Al_2O_3. *J. Phys. IV* **1997**, *7*, C2–935−936.

43 Kosmulski, M. The pH-dependent Surface Charging and Points of Zero Charge V. Update. *J.Colloid Interface Sci.* **2011**, *353*, 1–15.

44 Brydson, R.; Sauer, H.; Engel, W.; Thomas, J. M.; Zeitler, E.; Kosugi, N.; Kuroda, H. Electron Energy Loss and X-ray Absorption Spectroscopy of Rutile and Anatase: a Test of Structural Sensitivity. *J. Phys.: Condens. Matter* **1989**, *1*, 797–812.

45 Akita, T.; Tanaka, S.; Tanaka, K.; Kohyama, M. TEM and STEM Study of the Au Nano-particles Supported on Cerium Oxides. *Mater. Sci. Forum* **2010**, *654−656*, 2362–2365.

46 Akita, T.; Tanaka, K.; Kohyama, M. TEM and HAADF-STEM Study of the Structure of Au Nano-particles on CeO_2. *J. Mater. Sci.* **2008**, *43*, 3917–3922.

47 Akita, T.; Tanaka, S.; Tanaka, K.; Haruta, M.; Kohyama, M. Sequential HAADF-STEM Observation of Structural Changes in Au Nanoparticles Supported on CeO_2. *J. Mater. Sci.* **2011**, *46*, 4384–4391.

48 Hasegawa, T.; Kobayashi, K.; Ikarashi, N.; Takayanagi, K.; Yagi, K. Atomic Resolution TEM Image of The Au(001) Reconstructed Surface. *Jpn. J. Appl. Phys.* **1986**, *25*, L366–L368.

49 Kawasaki, T.; Takai, T.; Shimizu, R. Distorted Surface and Interface Structures of Catalytic Gold Nanoparticles Observed by Spherical Aberration-free Phase Electron Microscopy. *Appl. Phys. Lett.* **2001**, *79*, 3509–3511.

50 Kolb, D. M. Reconstruction Phenomena at Metal-electrolyte Interfaces. *Prog. Surf. Sci.* **1996**, *51*, 109–173.

51 Majimel, J.; Lamirand-Majimel, M.; Moog, I.; Feral-Martin, C.; Tréguer-Delapierre, M. Size-Dependent Stability of Supported Gold Nanostructures onto Ceria: an HRTEM Study. *J. Phys. Chem. C* **2009**, *113*, 9275–9283.

52 Takei, T.; Akita, T.; Nakamura, I.; Fujitani, T.; Okumura, M.; Okazaki, K.; Huang, J.; Ishida, T.; Haruta, M. Heterogeneous Catalysis by Gold. *Adv. Catal.* **2012**, *55*, 1–126.

53 Haider, M.; Rose, H.; Uhlemann, S.; Kabius, B.; Urban, K. Towards 0.1 nm Resolution with the First Spherically Corrected Transmission Electron Microscope. *J. Electron Microsc.* **1998**, *47*, 395–405.

54 Akita, T.; Tanaka, K.; Kohyama, M.; Haruta, M. HAADF-STEM Observation of Au Nanoparticles on TiO_2. *Surf. Interface Anal.* **2008**, *40*, 1760–1763.

55 Fujita, T.; Guan, P.; MacKenna, K.; Lang, X.; Hirata, A.; Zhang, L.; Tokunaga, T.; Arai, S.; Yamamoto, Y.; Tanaka, N.; Ishikawa, Y.; Asao, N.; Yamamoto, Y.; Erlebacher, J.; Chen, M. Atomic Origins of the High Catalytic Activity of Nanoporous Gold. *Nat. Mater.* **2012**, *12*, 1–6.